

IMAGING A BINARY STAR WITH A TWO-TELESCOPE
MICHELSON STELLAR INTERFEROMETER

H. M. DYCK

Department of Physics & Astronomy, University of Wyoming, Laramie, Wyoming 82071
Electronic mail: meldyck@uwoyo.edu

J. A. BENSON

Harvard-Smithsonian Center for Astrophysics, Cambridge, Massachusetts 02138
Electronic mail: benson@noao.edu

F. PETER SCHLOERB

Department of Physics & Astronomy, University of Massachusetts, Amherst, Massachusetts 01003
Electronic mail: schloerb@fcrao1.phast.umass.edu

Received 1994 October 18; revised 1995 April 3

ABSTRACT

Using a two-telescope Michelson stellar interferometer we observed the well known visual binary star ζ Her. By rapidly driving the optical delay line of the interferometer we were able to obtain temporally distinct interferograms from each component of the binary, preserving the image position information. This observation is presented as an illustration of a technique for imaging with two telescopes which we have named "delay-referenced interferometry." We discuss the implications our measurements for ζ Her and predict resolution limits for other binary systems. With the aid of a simple illustration, we argue that delay referencing is a useful technique for more complex systems when the object is contained entirely within the detector field of view and within the isoplanatic patch. We show how "snapshot" observations at a variety of interferometer orientations may be used in tomographic backprojection of delay-referenced fringes to generate an image of such sources. © 1995 American Astronomical Society.

1. INTRODUCTION

It is a widely accepted premise in multiple-telescope interferometry that high resolution imaging requires three or more telescopes (Pearson & Readhead 1984; Shao & Colavita 1992a), owing to phase errors generated within the interferometer and by the earth's atmosphere. Measurements of fringe amplitudes alone for a binary source are plagued by a persistent ambiguity of 180° in the orientation of the image of the source. For example, visibility observations of the spectroscopic binary α Equ made with the Mark III interferometer (Armstrong *et al.* 1992) have not directly yielded a complete binary solution. Rather, the relative orbit was obtained from the data through the application of smoothness constraints (Mozurkewich 1994). Closure phase techniques involving three or more telescopes (Jennison 1958; Rogers *et al.* 1974) are the method that has been developed for retrieving the visibility phases in the presence of large phase errors. Present plans for optical and infrared wavelength interferometric arrays pivot upon the assumption that closure phase can be made to work at those wavelengths (Armstrong 1994; Baldwin *et al.* 1994; McAlister *et al.* 1994).

More than a decade ago Koechlin *et al.* (1979) demonstrated that the 180° ambiguity in a binary star system could be removed from visibility data obtained with only two telescopes. They pointed out that the detailed behavior of the visibility within the spectral passband, $\Delta\lambda$, will be determined by the image geometry, and by spectrally dispersing the fringes within their passband, they determined the orien-

tation for the Capella binary system. Koechlin *et al.* conjectured that the dispersed fringe technique could be of general use for more complex sources than binary systems. Morancais & Nisenson (1988) have considered this technique for one dimensional observations and Schloerb (1990) has shown in numerical simulations that it is possible to reconstruct two-dimensional images from two-telescope visibility measurements with the dispersed fringe technique. Schloerb has pointed out that, for color-independent source geometry, the dispersed fringe observations can be used to provide phase constraints that are equivalent to closure phase constraints.

It is the purpose of this paper to resurrect these notions that two optical telescopes provide enough information to reconstruct useful images for certain classes of sources. We describe an elementary experiment which obtains a series of one-dimensional observations of a wide double star at a variety of orientations. For this illustration we were working in the image domain, where we showed that it is possible to preserve the relative orientation. The result is equivalent to having solved the phase problem in the complex visibility measurement. Our investigation differs from dispersed fringe techniques in that we make a direct measurement of its Fourier transform by observing the undispersed content of a relatively wide spectral passband. We note that Franz *et al.* (1992) carried out a similar experiment using the Koester prism interferometer on the fine guidance sensor on the *Hubble Space Telescope*, in order to detect the presence of

binary stars in the Hyades. Those authors did not exploit the imaging capabilities of the instrument.

We have chosen the well studied visual binary star ζ Her to provide ground truth information against which to compare our observations. The components of this system have been classified G0 IV for the primary (Keenan & McNeil 1989) and K0 V for the secondary (Struve & Ratcliffe 1954). The primary itself may be an unresolved spectroscopic binary (Baize 1976) with a separation smaller than 35 millarcsec (McAlister & Hartkopf 1988). This view has been disputed by Scarfe *et al.* (1983) based upon radial velocity studies. At optical wavelengths the visual pair has apparent magnitudes $V_P=2.90$ for the primary and $V_S=5.49$ for the secondary (Baize & Petit 1989). The combined magnitude at $2.2 \mu\text{m}$ is $K=1.27\pm 0.04$ (Neugebauer & Leighton 1969). To our knowledge, no individual magnitudes exist in the near infrared. Although we have chosen a very simple case for this experiment, we will argue that the technique has more general utility. Our observations were carried on IOTA, the Infrared Optical Telescope Array, described by Reasenberg (1990) and Carleton *et al.* (1994).

2. IMAGING A DOUBLE SOURCE WITH TWO TELESCOPES

Consider a pair of stars in a binary system, which is completely contained within the interferometer's field of view (FOV) during an observation. Owing to the angular separation of the two stars, the light from each travels a slightly different path through the interferometer. This results in different white-light fringe (WLF) positions for each component of the binary. Thus, as a function of optical delay through the interferometer, there will be two interference patterns—one for each star—separated by the difference in WLF positions. As noted by Franz *et al.* (1992), the two patterns result because the two stars are incoherent points in the image. The observed double interferogram is a linear combination of two interferometer transfer functions, scaled by the relative brightness of each source. In the “white light” limit (i.e., where the ratio of spectral bandwidth to wavelength $\Delta\lambda/\lambda \approx 1$) there will be one fringe corresponding to each star at their WLF positions. The path difference between the two white-light fringes will depend upon the angular separation between the stars, the position angle, and the interferometer baseline (Fomalont & Wright 1974). In practice, the spectral bandwidth will not be infinitely broad and there will be of order $2\lambda/\Delta\lambda$ fringes in the central lobe of the interferogram for each star, where the factor 2 arises because the interferogram is symmetric about the WLF position. If the stars are close together, or if the spectral bandwidth is narrow, or if the interferometer baseline is small, the central lobes of the two interferograms may overlap. For “wide” angular spacing and broad spectral bandwidths, the interferograms will be distinct and separate. In this case, the amplitude of each will be directly proportional to the brightnesses.

At IOTA, the optical delay line may be driven precisely, under computer control, at high speed through the WLF position for a given star. As the delay line passes through the WLF position, the detector produces a time-dependent signal which is proportional to the interferogram. When making

observations at $2.2 \mu\text{m}$, we normally drive the optical delay at a rate which generates a fringe frequency that is high compared to atmospheric noise frequencies. For an appropriately chosen binary star system, with both components always in the detector FOV, it is possible to drive the delay line such that it passes through the WLF positions for both stars during the data collection period. By recording the detector output, one can record the two interferograms as the delay line sweeps past the two WLF positions associated with the two stars.

If both stars are within the isoplanatic patch and if the delay line is moved at a high enough rate, a faithful one-dimensional “image” of the binary system will be obtained. The driven delay line technique will “freeze” the phase-perturbing effects of the atmosphere and yield a snapshot of the complete fringe packet. *With this technique, one may reference the fringes produced by different source components to a common fiducial component and preserve the relative positional information within the isoplanatic patch.* This is equivalent to the phase referencing technique (Peckham 1973) used in radio interferometry. We have named the procedure “delay referencing” to indicate that relative positional information is derived directly from a relative delay measurement. The delay referencing technique may be used to resolve the classical uncertainty of binary star interferometry, namely the orientation. Even when the above conditions have not been fully met, it will be possible to reproduce an image of the star under certain circumstances. For example, when the components of the binary are not both within the isoplanatic patch or when the delay line is not driven fast enough to freeze the atmospheric perturbations, a blurred image will result which is analogous to the seeing effects in ordinary long-exposure images. In this case, close binaries will not be resolved. However, when the angular separation is greater than the seeing angle, an image may still be obtained. This is equivalent to the case of narrow-angle astrometry using interferometers which has been described by Shao & Colavita (1992b).

3. DELAY-REFERENCED INTERFEROMETRY OF ζ HER

The observations reported here were made on UT 1994 June 9 with a telescope separation of 21.2 m on an approximately north–south baseline. A standard K filter ($\lambda=2.2 \mu\text{m}$, $\Delta\lambda=0.4 \mu\text{m}$) was used with two single-element InSb detectors operated in photovoltaic mode. The optical delay line was moved at a rate which produces a nominal fringe frequency of 100 Hz. An ideal interferogram for an unresolved source will contain approximately 10 fringes in its central lobe. The secondary component to ζ Her is sufficiently faint at K that its interferograms have a signal-to-noise ratio $S/N \approx 4$. At the present time, one of our detector systems suffers from a high level of microphonic noise and only the quiet detector was used to acquire data for this experiment. Fringe signals are displayed in real time on an oscilloscope and we could recognize two distinct fringe patterns in the first set of observations. In Fig. 1 we have shown several examples of the composite interferogram for the binary star. There is clear and strong evidence for the presence of a

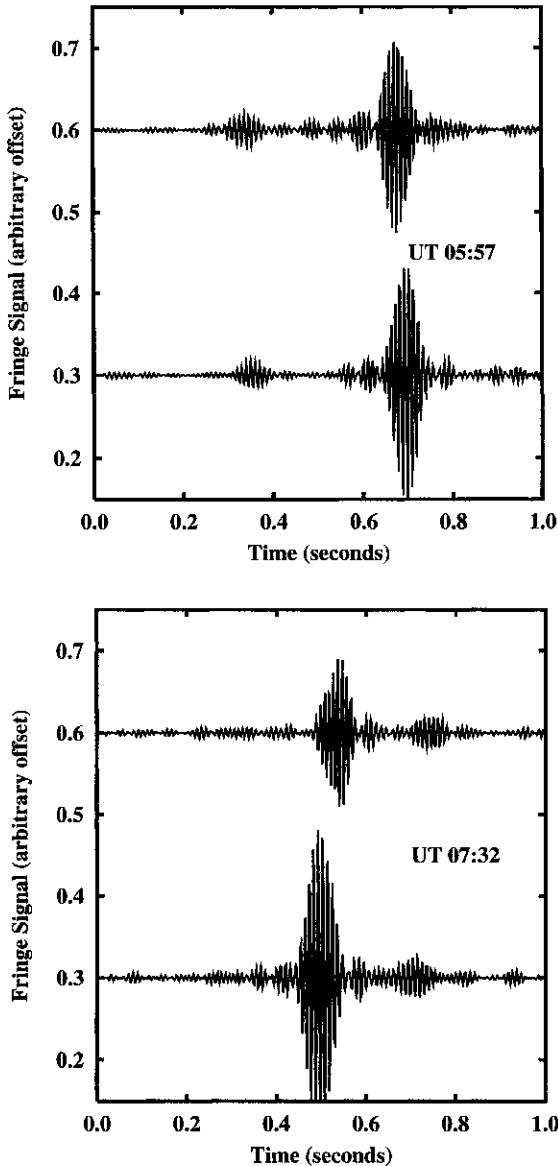


FIG. 1. Examples of interferograms of the visual binary ζ Her for two different observing times. Note the appearance of two interferograms in each scan, one corresponding to each component of the system. In the panel labeled UT 05:57, the optical delay line carriage was driven from north to south. The occurrence of the secondary interferogram before the primary one indicates that the secondary lies to the north of the primary. This is consistent with current orbital predictions. In the other panel, the optical delay was scanned in the opposite direction, so that the positions of the primary and secondary interferograms are reversed.

fainter companion in each of these interferograms. Further, in the figure panel labeled UT 05:57, we were scanning the delay line so that the zero-path position swept from north to south in the FOV. The appearance of the secondary star's interference pattern before the primary star's interference pattern is consistent with the current orbital predictions. In the panel labeled UT 07:32 we were scanning the delay line in the opposite sense and the relative positions of the secondary and primary interference patterns in the scan have been reversed. At the fringe rate selected, the atmospheric phase

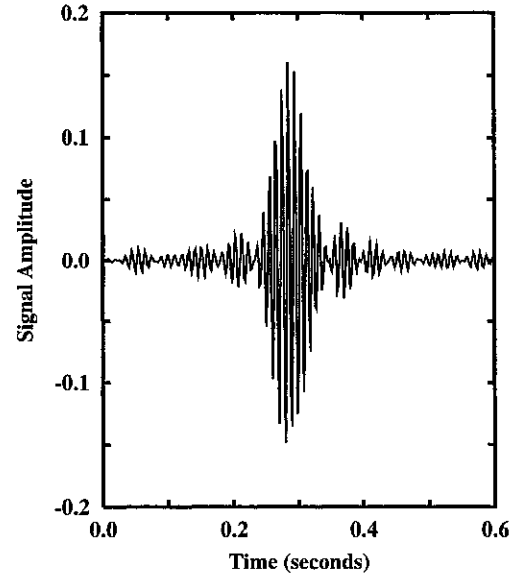


FIG. 2. An example of the interferogram produced by a single, unresolved star. This is the instrument point response or point transfer function.

fluctuations are not completely frozen, since the separation between interferogram signals for the primary and secondary ranges between 0.2 and 0.4 s. This results in noticeable fluctuations in the spacing and relative amplitude from one scan to the next. However, the phase fluctuations are not so large that they complicate the interpretation.

We alternated observations of ζ Her with observations of unresolved single stars to demonstrate that the double star observations were not an instrumental artifact. In Fig. 2 we have shown a typical example of one of these calibrator interferograms. This is an estimate of the interferometer point transfer or point response function. We inspected the single star interferograms on both sides of the position of the central fringe packet. In no case was there any evidence for a ghost interferogram, produced perhaps by a very large phase excursion, detector response effects, channel fringes within the interferometer, or any number of conspiring, perverse instrumental effects which might be interpreted as a companion. Thus, we have illustrated that it is possible to obtain the correct relative position of the star pair by using the delay-referenced interferometry technique, even though we are not strictly observing within the domain where there are no atmospheric effects that limit the measurement of relative delay.

4. DISCUSSION OF THE RESULTS

We have assumed that the primary and secondary components are individually unresolved by the interferometer so that the ratio of the amplitudes from the individual interference packets directly gives the flux ratio for the two components. From four separate sets of delay scans (80 interferograms total), we obtain a mean primary to secondary flux ratio at $2.2 \mu\text{m}$ $F_p/F_s = 6.9 \pm 0.2$. If we use the combined magnitude $K = 1.27 \pm 0.04$ (Neugebauer & Leighton 1969) with this flux ratio, we obtain $K_p = 1.42 \pm 0.05$ and

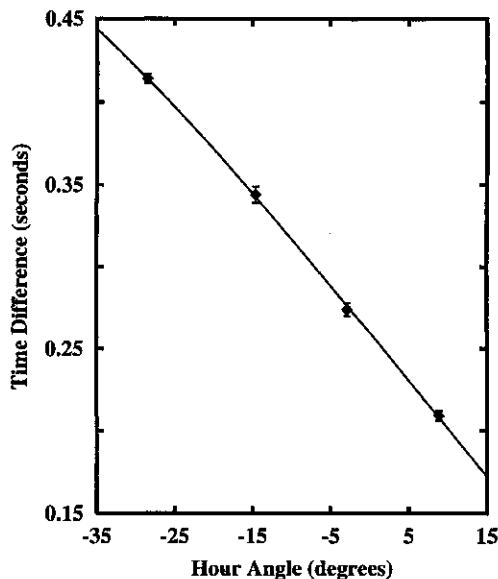


FIG. 3. A plot of the absolute value of the time difference between the WLF for primary and secondary components of the binary system as a function of hour angle. The solid curve is a model corresponding to $\rho=1.466\pm 0.005$ arcsec and $PA=63.7\pm 0.3^\circ$. The filled diamonds (\blacklozenge) are data, where the error bars are ± 1 standard deviation of the mean.

$K_S=3.51\pm 0.05$. Thus, the color difference for the secondary star is $V-K=1.98$, somewhat redder than the $V-K=1.83$ assigned to normal K0 V stars by Johnson (1966). Using the colors, we suggest that the spectral type of the secondary may be closer to K1 V, which is in good agreement with the estimate of Struve & Ratcliffe (1954), given the difficulty those authors had obtaining a spectrum of the secondary. In principle, we may also address the question of a companion to the primary; we have not done so because the problem is beyond the scope of this paper.

Owing to the apparent rotation of the interferometer baseline with respect to the line joining the binary pair during the night, we may use the observed variation of the time difference between primary WLF and secondary WLF to derive the position angle and separation. In Fig. 3 we have shown a plot of this variation (as the absolute value of the time difference in seconds vs hour angle in degrees) along with the best-determined model. The error bars on the time delay data are ± 1 standard deviation of the mean. Adopting the definition convention used by Fomalont & Wright (1974), we take B_x , B_y , and B_z to be the projections of the interferometer baseline onto the equatorial coordinate system. For a double source, the difference in optical delay between two close sources is

$$\begin{aligned} \Delta(OD) = & -(B_x \sin \delta \cos H + B_y \sin \delta \sin H \\ & - B_z \cos \delta) \Delta \delta \\ & - (B_x \cos \delta \sin H - B_y \cos \delta \cos H) \Delta H, \end{aligned} \quad (1)$$

where δ is the source declination, H is its hour angle and $\Delta\delta$ and ΔH are, respectively, the difference in declination and hour angle between the binary components. The delay between the two white light fringes, when the optical delay line

is driven at a speed which produces a desired fringe rate ν_D , is

$$\Delta t = - \frac{\Delta(OD)}{\nu_D \lambda}, \quad (2)$$

where λ is the wavelength of the observation. It may be seen from Eq. (1) that observation of the fringe delay over a range of hour angles will allow the observer to determine $\Delta\delta$ and ΔH . Using a linear least-squares analysis we have obtained $\rho=1.466\pm 0.005$ arcsec and $PA=63.7\pm 0.3^\circ$ from the observed data. The expected variation of fringe time difference with hour angle, computed from Eq. (2) using these parameters, is shown in Fig. 3. We determine the interferometer baseline vector by measuring the time of occurrence for the central fringe for stars with well determined positions which are scattered around the sky. Uncertainty from our baseline vector determination appears to be negligible compared to the other sources of error. Using the recent orbital elements from Baize (1976), we predict a position angle $PA=63.7^\circ$ and a separation $\rho=1.49$ arcsec for the secondary with respect to the primary for our observation epoch. Our observed position angle is in agreement with this prediction, although our separation is smaller than the prediction by significantly more than our estimated error. We expect that the differences are within the accuracy of the orbital predictions.

5. LIMITS FOR OBSERVING BINARY STARS

The binary system chosen for our illustration is not a particularly challenging one since the north-south component of the separation is of order 0.7 arcsec. Although this spatial resolution is not routinely available for images in the near infrared, it is easily obtainable with IOTA. It is of interest, indeed, to evaluate the limit for the kinds of observations reported here. We may proceed by defining a resolution criterion for composite response functions. With no sophisticated modeling it would be possible to recognize the existence of two equally bright components of a double source when the first zeros of their fringe packets are just touching. Since one can easily distinguish high S/N interferograms from components 2-3 times closer together, this criterion is somewhat conservative. With the K filter, there would be approximately ten fringes between WLF positions for the two components. Ten fringes corresponds to an optical delay difference of $22 \mu\text{m}$ at $2.2 \mu\text{m}$. We consider only the degenerate case for an interferometer with a purely north-south baseline (i.e., there is no east-west or elevation difference between the telescopes) where the star is observed at the zenith. In this case, it may be shown that the minimum observable declination separation would be

$$\Delta \delta = \left(\frac{\Delta(OD)}{B_z} \right) \cos L \quad (3)$$

radians, where L is the latitude of the interferometer. For an interferometer with a 40 m north-south baseline (approximately equivalent to IOTA at its maximum resolution), $\Delta\delta=0.11$ arcsec in the K filter. If we were observing with a J filter ($\lambda=1.25 \mu\text{m}$, $\Delta\lambda=0.4 \mu\text{m}$), then $\Delta\delta=0.04$ arcsec. At visible light wavelengths it should be possible to obtain $\Delta\delta$

$=0.005$ arcsec using such a technique. Thus, for example, at $1.25 \mu\text{m}$ one could resolve close binary star systems at the distance of the Taurus cloud (140 pc) with separations of order the distance between the earth and Jupiter. A survey could be carried out at the longest interferometer baseline by observing candidate stars over a range of hour angles and our demonstrated precision from this experiment is of order ± 0.005 arcsec. Moreover, if we had truly frozen the atmospheric phase fluctuations in our experiment, then even smaller errors would be possible.

6. THE GENERAL UTILITY OF DELAY-REFERENCED INTERFEROMETRY

It is a simple step to generalize this process to more complex systems. Each object will produce a composite interferogram which is a unique measure of its brightness distribution. If the observations “freeze” the phase-perturbing effects of the atmosphere and the instrument, then one can obtain a phase-accurate measure of the brightness distribution. It should be possible to fit model brightness distributions to arbitrarily complex sources, limited only by the final S/N in the composite interferogram, as long as the interferometer does not “resolve out” the structure, as discussed below. We illustrate this principal with a fourplex of point sources of different brightness, to be described in the following paragraphs.

The theoretical interferogram response, R , of the interferometer as a function of the delay, Δ , between the arrival of the wavefronts from the interferometer elements at the detector may be written:

$$R(\Delta) = 2\langle I \rangle + 2\Re \left\{ \int p(\sigma) e^{-i2\pi\sigma\Delta} \times \left[\int \int I_\sigma(\xi, \eta) e^{-i2\pi\sigma B\xi} d\eta d\xi \right] d\sigma \right\}, \quad (4)$$

where I_σ is the source intensity as a function of (spectral) wavenumber σ , $\langle I \rangle$ is the mean intensity averaged over wavenumber, $\Re(z)$ is the real part of z , $p(\sigma)$ is a function describing the wavelength response of the detector, B is the projected baseline length, and ξ and η are the (dimensionless) angular sky coordinates parallel and perpendicular to the projected baseline. By this choice of coordinate system the integration along the η axis is straightforward:

$$R(\Delta) = 2\langle I \rangle + 2\Re \left\{ \int p(\sigma) e^{-i2\pi\sigma\Delta} \times \left[\int s_\sigma(\xi) e^{-i2\pi\sigma B\xi} d\xi \right] d\sigma \right\}, \quad (5)$$

where $s_\sigma(\xi)$ is the strip-integrated brightness distribution of the source as a function of angular position on the sky, ξ , along the projected baseline. Now the Fourier transform of the brightness distribution $s_\sigma(\xi)$ is the visibility function, $V_\sigma(u)$:

$$V_\sigma(u) = \int s_\sigma(\xi) e^{-i2\pi u\xi} d\xi, \quad (6)$$

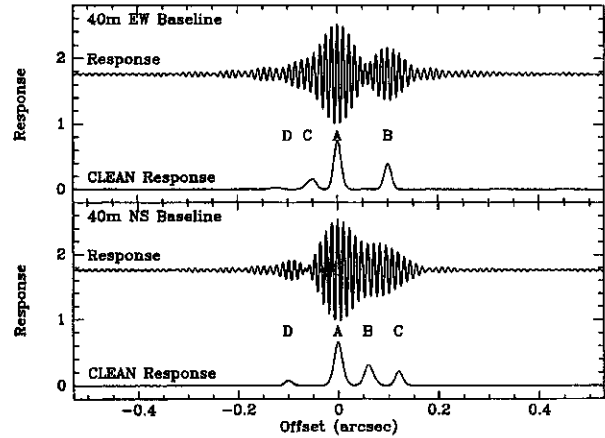


FIG. 4. Synthetic interferograms for two 40 m orthogonal arms of an interferometer for a source consisting of four components labeled A, B, C, and D. Also shown is the result of CLEANING these synthetic responses with the interferometer point source response.

where $u = \sigma B$, and with this result, the interferometer response in Eq. (5) may be rewritten:

$$R(\Delta) = 2\langle I \rangle + 2\Re \left[\int p(\sigma) V_\sigma(\sigma B) e^{-i2\pi\sigma\Delta} d\sigma \right]. \quad (7)$$

We now consider the case where the source brightness is independent of wavenumber, σ . If we further define the Fourier transform of the passband function as

$$P(\Delta) = \int p(\sigma) e^{-i2\pi\sigma\Delta} d\sigma \quad (8)$$

and apply the convolution theorem, then Eq. (7) may be written

$$R(\Delta) = 2\langle I \rangle + 2\Re \left(P(\Delta) \circ \frac{s(-\Delta/B)}{B} \right), \quad (9)$$

where \circ represents the convolution operator and P is revealed to be the response function of the instrument to a point source.

From Eq. (9), we see that the interferogram response of the interferometer to a gray source may be understood to be a convolution of the instrument’s response to a point source and the strip-integrated brightness distribution of the source on the sky. The information about the strip brightness distribution contained in $R(\Delta)$ is, of course, limited in important ways by the incomplete sampling of its’ Fourier transform, since the function $p(\sigma)$ does not fully sample all values of x . However, this is not an insurmountable problem for many sources since it is entirely analogous to the familiar situation of incomplete sampling of the UV plane in aperture synthesis. Several “deconvolution” algorithms have been constructed for this purpose (cf. Pearson & Readhead 1984) and, in this paper, we illustrate the use of one of them—the simple CLEAN algorithm—in the interpretation of interferogram data.

In Fig. 4, we show the synthetic responses of the IOTA detector system to a simple model source consisting of four point source components, A, B, C, and D, in the flux ratio 10:5:3:1. The secondary components (B, C, and D) are lo-

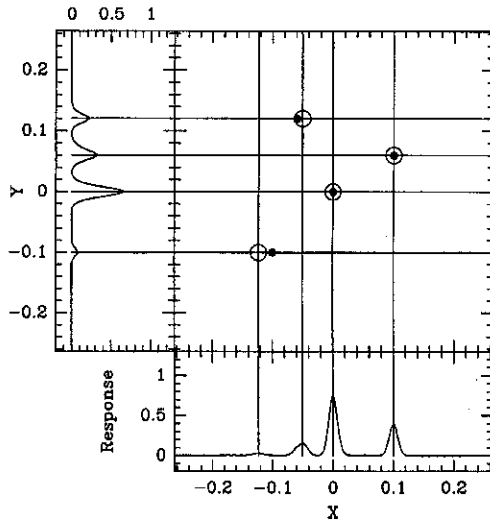


FIG. 5. A simple backprojection from the CLEANED brightness projections in the two orthogonal directions. The source components are located where lines of equal brightness intersect and are marked by open circles (O) for which the diameter indicates the approximate resolution. For comparison, the location of the original sources are shown as filled dots (●). Note that only the faintest component (component D) lies outside the resolution element.

cated at offset positions of $(0.10'', 0.06'')$, $(-0.06'', 0.12'')$ and $(-0.10'', -0.10'')$, respectively, relative to source A. In the top panel of Fig. 4 we show the synthetic interferogram of the source computed for a 40 m east–west baseline. Since the angular offset between components is directly related to the delay offset according to $\xi = -\Delta/B$, the x axis of the interferogram in the figure has been presented in terms of the angular offsets from the central source in order to clarify the connection between the observation and the source’s strip brightness distribution.

The result of deconvolving the synthetic interferogram with the CLEAN algorithm is also shown in the top panel for the 40 m east–west baseline. A similar set of calculations is shown in the bottom panel for the orthogonal 40 m north–south baseline. The locations of the four components are noted with letters A, B, C, and D. The CLEAN algorithm works reasonably well with this simple source model, despite the complex nature of the instrument’s point source response. Only two of the source positions, C and D, appear to be slightly biased in position for the east–west baseline and only source position D disagrees with its expected position by more than the resolution defined for the CLEAN response (set to approximately 2 fringes). Thus, the procedure of deconvolving the interferometer’s delay response to obtain an estimate of the strip-integrated brightness distribution of the source appears to be a reasonable one for this type of source.

It has long been appreciated that measurements of the strip brightness distribution in an astronomical source, such as those obtained above, may be used to reconstruct the full two-dimensional brightness distribution (cf. Bracewell 1979). Thus, given a procedure to obtain this information from the interferogram, we now discuss ways in which this type of data might be used in image reconstruction. In Fig. 5, we illustrate the fundamental principles involved by display-

ing the orthogonal CLEANED brightness projections, oriented with respect to the sky coordinates (now called X and Y) and back projected to produce a crude two-dimensional image. In this illustration, the source locations are given by the intersections of lines of equal brightness and are indicated in the figure by small circles. The original positions are shown for comparison by solid dots. We now see that the technique does a reasonable job of recovering the two-dimensional locations of the source components with respect to the primary component.

For sources more complex than a simple collection of points, the approach to image reconstruction must be correspondingly more complex. However, since the tomographic principles of image reconstruction from projected distributions are well established, there is a clear approach to imaging that makes direct use of this type of data. According to the “central slice theorem” of tomography (see Fraser *et al.* 1985), the Fourier transform of the projected (i.e., strip-integrated) brightness distribution of the source corresponds to a slice through the center of the two-dimensional Fourier transform of that brightness distribution. The interferogram response of an interferometer is related to the projected brightness distribution by a convolution operation, and following Eq. (9), the Fourier transform of the interferogram is a product of the visibility as a function of baseline length along the direction of the projected baseline, $V(\sigma B)$, and the detector bandpass function, $p(\sigma)$. Thus, the Fourier transform of the observed interferogram provides samples of the visibility along a slice through the UV plane and, by obtaining many such slices, a tomographic image may be constructed.

From an inspection of the data compression experiments on images in the paper by Fraser *et al.* (1985) one infers that more complex sources require a more complete sampling in the UV plane to produce a high fidelity image. The observing strategy would be to observe the source over a wide range of times, allowing the earth’s rotation to change the interferometer’s baseline projected length and direction. Snapshot observations will provide the necessary image slice information to permit tomographic reconstruction of structures in the image which are within the resolution of the interferometer. One complication is that, when there are more than a few fringes projected on the source, the interferometer will “resolve out” the structure. Indeed, our numerical simulations of high resolution observations of stars indicate that the interferometer is only sensitive to the edges of the stellar disk, where significant image power exists at spatial frequencies sampled by the interferometer. For structure on scales of the stellar diameter which are not sampled by the interferometer, a repeat of the procedure with smaller telescope separations is required to complete the data set so that all spatial frequencies are sampled.

Tomographic backprojections for such multiple slice data, as compared to the simple two-slice example given above, have the additional complication that one must be able to align each of the slices correctly with respect to all the others. Thus, a recognizable fiducial is required in each scan. This requirement will, of course, limit the applicability of the technique to particular classes of sources. In our view, two-

dimensional imaging using the delay-referenced interferometry technique will be particularly suited to bright, unresolved sources surrounded by fainter “fuzz” which could be in the form of companion sources (binaries, triples, and the like) or knots and streamers of luminous material. Recovery of simple structure on the surface of stars (extension of solar physics problems) may also be possible and is currently under investigation.

We gratefully acknowledge partial financial support from NSF Grant AST-9021181 to the University of Wyoming. This research has made use of the Simbad database, operated by the CDS, Strasbourg, France. We have had very helpful discussions with W. A. Traub, H. A. McAlister, S. T. Ridgway, and R. Millan-Gabet. We thank the referee for constructive comments about the delay-referencing technique.

REFERENCES

- Armstrong, J. T., *et al.* 1992, *AJ*, 104, 241
 Armstrong, J. T. 1994, *Proc. SPIE*, 2200, 62
 Baize, P. 1976, *A&AS*, 26, 177
 Baize, P., & Petit, M. 1989, *A&AS*, 77, 497
 Baldwin, J. E., *et al.* 1994, *Proc. SPIE*, 2200, 112
 Bracewell, R. N. 1979, in *Image Reconstruction from Projections*, edited by G. I. Herman (Springer, Heidelberg), p. 81
 Carleton, N. P., *et al.* 1994, *Proc. SPIE*, 2200, 152
 Fomalont, E., & Wright, M. C. H. 1974, in *Galactic and Extra-galactic Radio Astronomy*, edited by G. L. Verschuur and K. I. Kellerman (Springer, New York), p. 256
 Franz, O. G., *et al.* 1992, *AJ*, 103, 190
 Fraser, D., Hunt, B. R., & Su, J. C. 1985, *Optical Engineering*, 24, 298
 Jennison, R. C. 1958, *MNRAS*, 118, 276
 Johnson, H. L. 1966, *ARA&A*, 4, 193
 Keenan, P. C., & McNeil, R. C. 1989, *ApJS*, 71, 245
 Koechlin, L., Bonneau, D., & Vakili, F. 1979, *A&A*, 80, L13
 McAlister, H. A., & Hartkopf, W. I. 1988, *Second Catalog of Interferometric Measurements of Binary Stars*, Chara Contrib. No. 2 (Georgia State University, Atlanta)
 McAlister, H. A., *et al.* 1994, *Proc. SPIE*, 2200, 129
 Morancais, D., & Nisenson, P. 1988, *Optics Comm.*, 67, 39
 Mozurkewich, D. 1994, private communication
 Neugebauer, G., & Leighton, R. B. 1969, *Two-Micron Sky Survey, A Preliminary Catalog*, NASA SP-3047
 Pearson, T. G., & Readhead, A. C. S. 1984, *ARA&A*, 22, 97
 Peckham, R. J. 1973, *MNRAS*, 165, 25
 Reasenberg, R. D. 1990, *Proc. SPIE*, 1237, 128
 Rogers, A. E. E., *et al.* 1974, *ApJ*, 193, 293
 Scarfe, C. D., Funakawa, H., Delaney, P. A., & Barlow, D. J. 1983, *JRASC*, 77, 126
 Schloerb, F. P. 1990, *Proc. SPIE*, 1237
 Shao, M., & Colavita, M. M. 1992a, *ARA&A*, 30, 457
 Shao, M., & Colavita, M. M. 1992b, *A&A*, 262, 353
 Struve, O., & Ratchiffe, E. 1954, *PASP*, 66, 31